Structural Biology of Coronavirus Ion Channels

Francisco J. Barrantes

Biomedical Research Institute (BIOMED), Catholic University of Argentina (UCA)–National Scientific and Technical Research Council (CONICET), C1107AFF Buenos Aires, Argentina.

email: francisco_barrantes@uca.edu.ar

Keywords

Coronaviruses, COVID-19, SARS-CoV-2, cryo-electron microscopy, viroporins, viral ion channel proteins, structure-function correlations

Abstract (196 w)

Viral infection compromises specific organelles of the cell and readdresses its functional resources to satisfy the needs of the invading body. Around 70% of the coronavirus single-stranded (+)RNA genome encodes proteins involved in their replication and these viruses essentially take over the biosynthetic and transport mechanisms to ensure the efficient replication and trafficking of their virions. Some coronaviruses encode genes for ion channel proteins -the envelope protein E (orf4a), orf3a and orf8- which they successfully employ to master control of the endoplasmic reticulum-Golgi complex intermediate compartment, or ERGIC. The E protein, one of the four structural proteins of SARS-CoV-2 and other coronaviruses, assembles its transmembrane protomers into homo-pentameric channels with mild cationic selectivity. Orf3a forms homo-dimers and homo-tetramers. Both carry a PDZ-binding domain lending them the versatility to interact with more than 400 target proteins in the infected host cells. Orf8 is a very short 29-amino-acid single-passage transmembrane peptide that forms cation-selective channels when assembled in lipid bilayers. This review addresses the contribution of biophysical and structural biology approaches that unravel different facets of coronavirus ion channels, their effects on the cellular machinery of infected cells, and some structure-functional correlates with ion channels of higher organisms.

Introduction and Background

Only a few weeks after the outbreak of the coronavirus (CoV) disease 2019 (COVID-19) pandemic, biophysical studies produced atomic scale data on key structures of the causative agent, severe acute respiratory syndrome coronavirus 2 (SARS-CoV-2). This attests to a very positive reaction of the scientific community in tackling a biomedical problem of unprecedented proportions. Structural biology was the first scientific discipline to apply powerful biophysical methods and produce solid data in attempts to understand the pathogenesis of the disease and search for its biomedical remediation (Barrantes, 2021).

From a genomic perspective, SARS-CoV-2 belongs to the same category of positive strand (+)RNA viruses as hepatitis C, chikingunya and Zika viruses. From a taxonomic viewpoint, SARS-CoV-2 belongs to the subfamily *Coronavirinae* in the *Coronaviridae* family that comprises four genera: α, β, γ and δ (Gonzalez *et al.*, 2003, Letko *et al.*, 2018). Coronaviruses (CoVs) pack inside their envelope between 26 and 32 kilobases of single-stranded positive-sense (+) RNA. CoVs were first identified in the late 1970's in electron microscopy (EM) studies of negatively stained specimens and their name was coined after the fuzzy solar corona appearance surrounding the spherical virion envelope (Almeida & Tyrrell, 1967), which we now know stems from the coverage of the envelope with spike (S) protein copies, one of the four structural proteins in these viruses. The highly pathogenic avian bronchitis virus was discovered in the early 1930's (Estola, 1970) but it was not known until decades later that it belonged to the γ genus of the *Coronaviridae* (Gonzalez *et al.*, 2003). CoVs cause mild to severe respiratory,

enteric and neurological diseases in species ranging from avians to mammals (Lai & Cavanagh, 1997, Cui *et al.*, 2019, Woo *et al.*, 2014).

The first study to identify a CoV infection in humans is attributed to Hartley and coworkers, who found antibodies to mouse hepatitis virus (MHV) in the serum of affected patients (Hartley *et al.*, 1964). A total of seven CoVs (HCoVs) have since been identified. HCoV-OC43, HCoV-293, HCoV-NL63 and HKU1-CoV generally cause mild respiratory diseases, mainly forms of the common flu along with other viruses with tropism for the nasal and upper respiratory tract mucosae. A second category of HCoVs comprises the highly pathogenic SARS-CoV and MERS-CoV, the etiological agents of the severe acute respiratory syndrome (SARS) and the Middle East respiratory syndrome (MERS), responsible for the 2003 and 2012 epidemics, respectively, and SARS-CoV-2, the causative agent of the current COVID-19 pandemic.

The structural-functional correlations of SARS-CoV-2 ion-channel proteins and their comparison with those of other pathogenic CoVs have still not been fully characterized. This is a needy area for investigation, particularly because these proteins are purported to fulfill a role in infected cells, with possible implications for interventions that interfere with viral replication. This short review discusses the topic of ion channel-forming protein structure in CoVs in general and in SARS-CoV-2 in particular, in an attempt to put the subject in perspective both from molecular biology and phylogenetic standpoints and to call attention to their potential as targets for prophylactic and/or therapeutic interventions.

Comprehensive reviews on the biological and evolutionary (Li *et al.*, 2020), epidemiology (Su *et al.*, 2016), clinical (Richardson *et al.*, 2020, Guan *et al.*, 2020),

microbiological (Fung & Liu, 2019) and physicochemical aspects (Scheller *et al.*, 2020) and structure (Harrison, 2015, Tortorici & Veesler, 2019) of CoVs have appeared. The reader is also referred to the reviews on the recent contribution of biophysics and structural biology to current advances in COVID-19 (Barrantes, 2021) and the new possibilities for repurposed drugs (Barrantes, 2020, Cavasotto & Di Filippo, 2021, Cavasotto *et al.*, 2021) in handling the current pandemic.

Overall Structure of CoVs

A common characteristic of members of the *Coronaviridae* is the spiky appearance of the capsid (Neuman *et al.*, 2006, Neuman & Buchmeier, 2016, Wrapp *et al.*, 2020). Contemporary cryo-EM images of the SARS-CoV-2 virion isolated from the supernatant of infected cells show roughly spherical bodies with a diameter of 91 ± 11 nm (Ke *et al.*, 2020), i.e. very similar to other CoVs. Around 70% of the SARS-CoV-2 genome encodes proteins involved in RNA replication, the rest of the genome coding for structural and non-structural proteins. Besides the aforementioned S protein, CoVs have three additional structural proteins: nucleocapsid (N), envelope (E) and membrane protein (M), 16 non-structural proteins and 8 open reading frame (orf) accessory proteins (Díaz, 2020).

N, the nucleocapsid protein, resides together with the RNA genome in the ribonucleoprotein (RNP) core inside the envelope. The N protein chaperones and protects the genomic RNA. The M protein is an integral membrane glycoprotein that contributes to adapting a region of the endoplasmic reticulum-Golgi complex intermediate compartment (ERGIC) membrane for virus assembly and thus defining the

shape of the viral envelope. When expressed alone, M accumulates in the Golgi complex, but when expressed together with the E protein, virus-like particles akin to authentic virions in size and shape are assembled. This observation has led to the idea that the M and E proteins constitute the minimal building blocks for envelope formation (de Haan *et al.*, 1999).

Viral Ion Channel-forming Proteins (Viroporins)

In recent years X-ray crystallography, transmission EM and cryo-EM and nuclear magnetic resonance (NMR) techniques have been applied to study the structure of some viral ion channel-forming proteins, also termed "viroporins" (Liao *et al.*, 2006, Fischer & Hsu, 2011). The name, partly borrowed from the bacterial β-barrel porins, alludes to their ability to act as ion-conducting pores in membrane bilayers, but in fact they are more elaborate than this, exhibiting e.g., ion selectivity. In silico studies using sequence-based molecular modelling and homology modelling have provided complementary insights into these structures, finding common architectures as well as diversity (see e.g. review in ref. (OuYang & Chou, 2014)). Viral viroporins exhibit a low degree of homology with ion channels of prokaryotic or eukaryotic origin if one considers their overall structure, although their transmembrane (TM) regions do bear some resemblance to the corresponding regions in ion channels of higher organisms (Fischer & Hsu, 2011), as analysed in the section on the evolution of these proteins.

One of the first descriptions of ion channel protein in viruses dates back to the early 1990's, when the matrix M2 protein of influenza virus was shown to confer ion permeability on monovalent cations upon heterologous transfection of *Xenopus* oocytes

(Pinto *et al.*, 1992). Subsequently it was demonstrated that this applies to influenza A and B viruses, which also display permeability for protons, whereas the M2 proteins of influenza C and D viruses exhibit selectivity for chloride ions, with some permeability for protons (see review in (To & Torres, 2019)).

In between the genes coding for the S protein and those for other viral envelope genes, the CoV RNA genome contains a locus conserved throughout the entire family. In the SARS-CoV genome, this region includes a complete or truncated open reading frame (ORF) (Zhang *et al.*, 2014) containing the gene encoding the E protein, also termed orf4a and orf3a and orf8a, three proteins that form ion channels (Castaño-Rodriguez *et al.*, 2018). CoVs MERS-CoV, HCoV-229E, HCoV-OC43 and porcine epidemic diarrhoea virus (PEDV) encode two such ion channel-forming proteins (To *et al.*, 2016, Castaño-Rodriguez *et al.*, 2018).

The small E protein (orf4a): Pentameric Structure and Membrane Topology

E is the smallest of the four structural proteins of CoVs. It is only 76 to 109-amino acids-long (Pervushin *et al.*, 2009). It is an integral membrane protein present in sub-stoichiometric quantities relative to other proteins embedded in the envelope bilayer membrane, and whose precise functions are still not fully known, except that its transmembrane domain (TM) possesses ion channel properties and is probably involved in virion assembly (Siu *et al.*, 2008) and virion release from infected cells (reviewed in (Schoeman & Fielding, 2019)). This has been documented for MHV, its expression in *E. coli* leading to increased permeability, growth arrest, and ultimately cell lysis (Madan *et al.*, 2005). The genome of SARS-CoV (Liao *et al.*, 2013), MERS-CoV (Surya *et al.*,

2015), and IBV, the highly pathogenic avian infectious bronchitis from the γ-CoV genus (To *et al.*, 2017), also code for E proteins. E possesses a short hydrophilic amino-terminal domain exposed to the cytoplasmic compartment of the host cell (Maeda *et al.*, 2001, Raamsman *et al.*, 2000), and a relatively long (25 amino acid stretch) TM domain. The TM domain of the E protein is highly conserved among CoVs, with ~91% sequence identity and 98% sequence similarity (Cao *et al.*, 2020).

The exact topology of E relative to the membrane is still an ongoing debate. Two amino acids are the main contributors to the hydrophobicity of the TM domain: valine and leucine (Wu *et al.*, 2003). The TM domain is followed by a long hydrophilic carboxy-terminus (Ye & Hogue, 2007) that possesses three cysteine residues suggested to play a role in the association of E with the spike glycoprotein S (Wu *et al.*, 2003). Expression of the SARS-CoV E protein in Vero E6 cells showed that it is N-glycosylated and that the two membrane-spanning domains comprise amino acid sequences 11-33 and 37-59, i.e. with a short loop between the two (Chen *et al.*, 2009). When analysing the TM region of E, one should consider the two possible loci inhabited by this protein: i) its native viral envelope bilayer lipid membrane and ii) the host cell intracellular membranes. In the former case, the E protein has been proposed to traverse the viral lipid bilayer as a single-passage helix (Raamsman *et al.*, 2000) or a double-passage helix (Raamsman *et al.*, 2000, Maeda *et al.*, 2001, Chen *et al.*, 2009). During the replication cycle in the host cell, E is mainly localized at the sites of viral replication, i.e. ER, Golgi and ERGIC membranes. Recombinant CoVs lacking the E protein show significantly lower viral titres / propagation-incompetent progeny, suggesting the importance of E in virion production and maturation (Schoeman & Fielding, 2019). E from infectious

bronchitis virus (IBV) has been reported to cross the Golgi membranes just once, with the N-terminus facing the Golgi lumen and the C-term facing the cytoplasm (Corse & Machamer, 2000), whereas E from MHV has been purported to traverse the lipid bilayer twice, with both the N- and C-termini exposed to the cytoplasmic compartment, which is topologically equivalent to the interior of the virion (Maeda *et al.*, 2001). A further proposal indicates that the SARS-CoV E TM region contains a 12 amino acid-long hairpin, which these authors indicate is capable of deforming lipid bilayers by increasing their curvature, a process that would occur during virion budding from the infected cells (Arbely et al., 2004). The NMR data of Torres and coworkers (Li et al., 2014) appeared to confirm the suggestion of a hairpin-like structure formed by two helices joined by a less ordered segment in the SARS-CoV E monomer. Subsequent work from the same group indicated that the E monomers possess only one membrane-embedded α-helical segment.

In terms of their oligomeric organization, a molecular modelling exercise led Torres and coworkers to suggest that the TM segments of SARS-CoV E protein monomers adopt a pentameric structure (Torres *et al.*, 2005). NMR later led to experimentally-supported models of SARS-CoV E protein structure (Pervushin *et al.*, 2009, Surya *et al.*, 2018, Li *et al.*, 2014).

---------- Figure 1 near here ----------

Figure 1A shows a model of the SARS-CoV E protein monomer obtained by solid-state NMR spectroscopy in detergent-lipid micelles. The E recombinant protein was expressed in bacteria and the lowest-energy structure was calculated (Li *et al.*, 2014). A long straight α-helix, the purported channel-forming domain, is joined through a flexible

linker domain (residues 46-54) to a short (residues 55-65) peripheral C-terminal helix that bends obliquely with respect to the longer helix and to the ion channel pore main axis (see Figure 2) at the level of residue Y42. Subsequent NMR studies in lauryl-myristoyl-phosphatidyl glycerol micelles (LMPG), showed the monomer (residues 8-65) to consist of three segments, with the two α-helices penetrating the bilayer and an overall shape resembling a fishing hook (Figure 1B).

The homo-oligomer of protein E is apparently self-generated through specific amino acid linear motifs of 5 copies of the monomer, as suggested for the human coronavirus HCoV-OC43 (Stodola *et al.*, 2018). Figure 2 draws a comparison between the E proteins of the two related viruses, SARS-CoV and SARS-CoV-2. The model of the SARS-CoV protein is derived from the NMR study in LMPG micelles (Surya *et al.*, 2018) and that of the SARS-CoV-2 E structure is derived from NMR data at 2.4 Å resolution of the protein reconstituted in ERGIC-mimetic liposomes containing phosphocholine, phosphoethanolamine, phosphatidylinositol, phosphoserine and cholesterol (Mandala *et al.*, 2020). The NMR structures depart from an ideal α-helical geometry, apparently due to deformations produced by three Phe residues stacked between the helical chains lining the narrow pore. The blocker hexamethylene amiloride binds to polar amino acid residues in the amino-terminal lumen of the pore. For comparative purposes between the liposomes made up of dimyristoyl-phosphocholine (DMPC):dimyristoyl-phosphoglycerol (DMPG) membranes were employed.

The ring of TM segments forming the SARS-CoV-2 protein E ion channel proper is also a pentameric bundle, but the helices run perpendicular to the membrane plane, whereas in the SARS-CoV E protein the homologous chains of the five monomers are assembled

into a pentameric body with an inner ring of TM α-helical segments (residues 15-45) tilted by ~15˚ relative to the axis of the central ion permeation pathway. (Figure 2, *top panel*). The most striking difference between the SARS-CoV and SARS-CoV-2 ion channel is the simpler architecture of the latter, with a bundle of straight α-helical chains forming a single ring, contrasting with the two helical rings in SARS-CoV. Since the two proteins share ~92% sequence homology, the possibility arises that the differences in structure of the membrane-associated region is partly due to the different media used in the NMR studies. A pentameric structure has also been proposed for the E protein of MERS-CoV (Surya *et al.*, 2018).

---------- Figure 2 near here ----------

In functional terms, early studies using planar lipid bilayers showed that synthetic peptides corresponding to the SARS-CoV E protein form ion channels in planar lipid bilayers with selectivity for permeating monovalent cations over monovalent anions (Wilson *et al.*, 2004). The E protein of SARS-CoV was also found to modify the permeability of *E. coli* membranes when expressed under reducing conditions, under which E adopts a monomeric state, whereas non-reducing conditions rendered the E protein in dimeric and homo-trimeric forms (Liao *et al.*, 2004). Reduction exposed two cysteine residues essential for S-S bond-mediated oligomerization; the changes in permeability were therefore attributed to the exposure of the cysteine residues, although no distinction could be established between the direct or indirect nature of the permeability changes using planar lipid bilayers (Verdiá-Báguena *et al.*, 2012). The E channel displays monovalent cation selectivity (Westerbeck & Machamer, 2019), although it has also been reported to permeate Ca^{2+} (Nieto-Torres *et al.*, 2015). Ion conductance can be blocked by hexamethylene amiloride, but not by amiloride, a drug that

inhibits viral replication of some synthetic E proteins from CoV (Pervushin *et al.*, 2009). Based on the conductance properties of E in planar bilayers (Wilson *et al.*, 2004) or upon transient expression in *Xenopus* oocytes and yeast systems, E was suggested to form non-selective channels for monovalent cations, although in the latter case Li^+ partially reduced inward currents (Zhang *et al.*, 2014). As observed with orf3a, viral production diminished when protein E expression was abrogated by applying siRNA to infected cells (Zhang *et al.*, 2014). The E protein of the new SARS-CoV-2 reconstituted in lipid bilayers with a composition reported to mimic that of the ERGIC membrane has recently appeared, showing that the ion channel displays a mild cationic permeability, which can be blocked by hexamethylene amiloride and amantadine binding to polar residues shallowly located at the N-terminal lumen (Mandala *et al.*, 2020) thus confirming earlier work on the inhibitory action of this drug on the viral channel (Pervushin *et al.*, 2009).

In vitro experiments have shown that the lipid composition of the host planar bilayer modulates ion conductance of the SARS-CoV E protein channel (Verdiá-Báguena *et al.*, 2012). Lipid charge was also found to play a role: the E protein showed no cation selectivity in uncharged lipid membranes, whereas negatively-charged lipids result in mild cationic selectivity (Verdiá-Báguena *et al.*, 2012). The charge of the ionizable groups of the E protein, as well as those from host lipids like diphtanoyl phosphatidylserine, was found to play a role in channel conductance (Verdiá-Báguena *et al.*, 2013).

Mutagenesis of amino acid residues in the hydrophobic TM domain of the E protein alters virus replication, which is restored upon re-establishing the α-helical structure (Ye & Hogue, 2007). Helix-restored E protein is more sensitive to treatment with

hexamethylene amiloride, a drug that inhibits the HIV Vpu virus ion channel and the E protein channel from human HCoV-229 and rodent MHV, but not avian IBV (Wilson *et al.*, 2006). Mutations N15A and V25F in the TM region of SARS-CoV E protein were reported to abrogate ion conductance (Verdiá-Báguena *et al.*, 2012).

Orf3a

SARS-CoV orf3a is a much larger -274 amino acids long- viral ion channel protein; it possesses three transmembrane domains. Initially described as a structural protein unique to the SARS-CoV (Shen *et al.*, 2005), it was subsequently reported that the orf3a protein from the same virus, coined by these authors as U274, was a nsp that interacted with the M, E and S structural proteins and orf7/U122 (Tan *et al.*, 2004). Recombinant SARS-CoV orf3a protein can form a homo-tetramer complex in orf3a-transfected cells (Lu *et al.*, 2006, Marquez-Miranda *et al.*, 2020). A tetramer consisting of four TM segments each has also been proposed using structure prediction computational approaches (Wang *et al.*, 2012). When expressed in *Xenopus* oocytes, SARS-CoV orf3a is a K^+-sensitive channel that can be efficiently inhibited by Ba^{2+}. Similarly, ion channel activity is generated upon transfection of porcine epidemic diarrhoea virus (PEDV) into *Xenopus* oocytes or yeast cells (Wang *et al.*, 2012). If cells are transfected with siRNA, thus suppressing orf3a expression, infection with SARS-CoV replication is not affected, but virion release is (Lu *et al.*, 2006). Synthetic peptides corresponding to each of the constituent TM segments of orf3a were reconstituted into artificial lipid bilayers. When the three peptides were assembled in a 1:1:1 mixture, ion channel activity was observed, but either TM domains 2 or 3 were required to induce currents: TM 1 failed to do so.

Full-length orf3a expression showed weak cationic selectivity and rectification (Chien *et al.*, 2013).

Recently, SARS-CoV-2 orf3a was heterologously expressed in *Spodoptera frugiperda*, reconstituted in liposomes and single-channel currents recorded from excised patches. (Kern *et al.*, 2020). Electrophysiologically, orf3a behaved as a cation channel with a large single-channel conductance (375 pA) with modest selectivity for Ca^{2+} and K^{+} over Na^{+}. The channel was not blocked by Ba^{2+} as is the case with the SARS-CoV channel (Lu *et al.*, 2006) nor inhibited by the small drug emodin.

Kern et al. also employed cryo-EM to image the apo-form of the orf3a dimeric and tetrameric forms reconstituted in lipid nanodisks. SARS-CoV-2 appears as a homo-tetramer in which each monomer of the dimers contributes with three TM segments arranged in clockwise fashion, making a total of 6 membrane-spanning domains per dimer (Figure 3A,B). Dimers are joined by a covalent S-S bond distended between homologous residues Cys-133 in each dimer in the in silico model produced by (Marquez-Miranda *et al.*, 2020) (Figure 3B) or residues W131, R134, K136, H150, T151, N152, C153 and D155 in the recent molecular modelling studies of Cavasotto and coworkers (Cavasotto & Di Filippo, 2021, Cavasotto *et al.*, 2021), bringing the total number of TM helices to 12 and thus making this the largest and most elaborate viral channel protein known to date. The ~ 2.9 Å resolution structure cryo-EM of SARS-CoV-2 (Kern *et al.*, 2020) is very similar to that of the orf3a channel structure of SARS-CoV orf3a (Lu *et al.*, 2006), corroborating the structural homology between several of the molecular constituents of these two human pathogenic viruses of the seven known to date (Barrantes, 2021). The all-helical TM region of the protein, with a length of ~ 40 Å,

adopts a peculiar novel topography in the lipid bilayer, whereas the cytosolic domain of the dimer (~ 30 Å) is formed by two β-sandwiches (Figure 3C). The novel ion channel structure possesses two potential ion pores, one in each dimer; the walls of the ion channel proper are lined by the TM 1 and 2 of each monomer (Figure 3C). The extracellular-facing end of the ion channel exhibits a narrow bifurcated pore reminiscent of the structure of vestibules in ion channels of higher organisms. This outer portion of the channel leads to a large polar cavity open to the cytosol. The orf3a structure was captured by cryo-EM in a conformation tentatively corresponding to a tetramer, and ascribed by the authors to the closed or inactivated state (Kern *et al.*, 2020). A tubular electron-dense region potentially corresponding to lipid acyl chains was partially resolved in between the TM helices.

---------- Figure 3 near here ----------

Interestingly, the molecular model using the cryo-EM data of the orf 3a protein (PDB 6XDC) (Marquez-Miranda *et al.*, 2020) disclosed the presence of Cl^- binding sites inside the ion permeation pathway of SARS-CoV-2 orf3a.

Orf8a

Information on Orf8a is still very scanty. It is a Cys-rich 29 amino acid-long single-passage TM peptide present at least in SARS-CoV. Orf8a forms cation-selective ion channels with a conductance close to 9 pS when assembled in lipid bilayers in several putative oligomeric forms, from tetramers to hexamers (Chen *et al.*, 2011). In silico calculations suggested that the first 22 amino acids of the single-TM domain of orf8a forms a homo-pentameric bundle (Hsu *et al.*, 2015). The pentameric bundle was also

purported to exhibit weak cation selectivity attributable to hydrophilic and hydrophobic stretches of amino acids in the channel lumen.

Contribution of Viral Ion Channel Proteins to Pathogenesis

SARS-CoV orf3a has been implicated in viral release, inflammasome activation and cell death, and its deletion reduces viral titres and morbidity in model systems (Freundt et al., 2010). E downregulates the type-1 interferon (IFN) receptor by inducing serine phosphorylation of the IFN α-receptor subunit 1 degradation motif and increasing the receptor ubiquitination (Minakshi et al., 2009).

The fact that a large proportion (>70%) of CoVs genome, including that of the SARS-CoV-2, is devoted to RNA replication dictates the preferential intracellular tropism of the virus to the biosynthetic machinery of the cell. Viral proteins are initially synthesized at the endoplasmic reticulum (ER) but most of the posttranslational modifications occur at the overlapping interface of the ER and the Golgi complex, the ERGIC zone. Indeed, labelling of the E protein with Rab-1, a cytochemical marker of the intermediate compartment and the ER, showed the accumulation of MHV CoV-A59 E protein in the ERGIC region of the cell; electron microscopy provided further evidence that E induces formation of tubular structures and induces curvature of the pre-Golgi membranes and subsequently alters the Golgi complex membranes (Raamsman *et al.*, 2000, Nieto-Torres *et al.*, 2015). E is purported to confer stability to the viral membrane and contribute to the later stages of the virion cycle in the infected cell -the assembly and the budding processes (Neuman *et al.*, 2011). E assembles by budding into the lumen of the early Golgi compartment (Westerbeck & Machamer, 2019).

Alanine scanning mutagenesis studies of the extramembrane domain of E have shown that certain mutations impair viral assembly and maturation, i.e. morphogenesis of MHV virions (Fischer *et al.*, 1998, Siu *et al.*, 2008). Although according to some authors (Venkatagopalan *et al.*, 2015) E does not traffic to the cell surface, avian IBV E protein interacts physically with the M protein and is able to retain M in the compartment it resides in (Lim *et al.*, 2001). In SARS-CoV this interaction is postulated to take place through the hydrophobic TM domains (Chen *et al.*, 2009). Propagation and shedding of SARS-CoV virus-like particles (VLP) requires the co-expression of E and N proteins together with the M protein (Siu *et al.*, 2008).

In addition to these roles in the assembly, trafficking and shedding of virions, the E protein is also involved in the stimulation of the immune response in the infected organism. The evolutionary conservation of the E protein among CoVs (Cao *et al.*, 2020) makes it an interesting candidate for vaccine development, and therefore knowledge of its surface epitopes is of biological and biotechnological importance. A step in this direction is the tentative mapping of the surface epitopes of SARS-CoV-2 E protein based on the structure of SARS-CoV (Tilocca *et al.*, 2020) (Figure 4). Polyclonal antibodies that recognize the N-terminal 19 amino acid residues of SARS-CoV E protein inhibit its ion current ability (Wilson *et al.*, 2004).

---------- Figure 4 near here ----------

Ion channel activity resulting from expression of CoV viroporins induces stress responses and activates proinflammatory pathways, and can lead to cell death (Minakshi *et al.*, 2009). In vitro, expression of SARS-CoV orf3a protein in the pulmonary epithelial cell line A549 upregulates expression of intracellular and secreted levels of

the three subunits of fibrinogen (Tan *et al.*, 2005). Infection of Vero E6 cells with SARS-CoV leads to apoptosis, which in turn triggers a virus-initiated cytopathic effect (Yan *et al.*, 2004). Other pathogenic changes include rearrangement of the membrane - accumulation of intracellular vesicles- Golgi fragmentation, and cell death induced by SARS-CoV orf3a, which is reduced upon deletion of orf3a (Freundt *et al.*, 2010). The virus also downregulates the signalling pathway inositol-requiring enzyme 1 (IRE-1) of the unfolded protein response (DeDiego *et al.*, 2011). Most recently the orf3a protein of the new SARS-CoV-2 has also been shown to induce apoptosis in various cell lines in vitro. The apoptotic process involves the activity of caspase-8, i.e. following the so-called extrinsic pathway, which induces the release of mitochondrial cytochrome c and caspase-9 activation; the levels of apoptosis were, however, lower than those induced in Vero E6 cells by SARS-CoV (Ren *et al.*, 2020).

Another expression of the pathogenic effects induced by SARS-CoV E protein is the increase in permeability of the ERGIC/Golgi membrane leading to the cytosolic release of Ca^{2+} with the concomitant activation of the NLRP3 inflammasome and induction of interleukin 1β (IL-1β) production (Nieto-Torres *et al.*, 2015). When (+)RNA viruses like the CoVs utilize the host-cell ERGIC membranes to reproduce their genomes, they modify this membrane complex to produce a structurally different organelle, the replication complex or replication organelle (Snijder *et al.*, 2020). This modified intermediate membrane compartment is characterized by the appearance of double-membrane vesicles (DMV) ~250-300 nm in diameter where the double-stranded RNA is copied into new (+)RNA genomes (Figure 5). How is the nascent genomic (+)RNA released from inside the DMVs into the cytosol? A recent cryo-EM tomography study of

cells infected with SARS-CoV-2 and other CoVs like MHV identified a pore traversing the two adjacent lipid bilayers of the DMVs. The pore is formed by six copies of the non-structural protein nsp3, essential for viral replication (Wolff *et al.*, 2020).

---------- Figure 5 near here ----------

Analogous structures called necked spherules can be observed in cells infected with other (+)RNA viruses like Zika (flavivirus), chikungunya (alphavirus) and nodaviruses. In the latter case, RNA replication organelles were imaged by cryo-EM tomography in the outer mitochondrial membrane opening towards the cell cytoplasm. The spherule neck appears as a ring containing 12 copies of the nodavirus RNA replication protein A (Unchwaniwala *et al.*, 2020).

CoV pathogenesis is intimately related to the ability of the infective viruses to hijack the various molecular effectors required to bind to, enter, replicate their RNA, assemble, and be released from the host cell. Viral assembly and intracellular migration is tightly coupled to the ERGIC cellular machinery and its vesicle-mediate transport. Expression of E protein from avian IBV has recently been discovered to induce neutralization of Golgi pH, altering the secretory pathway through interaction with host cell factors, thereby protecting IBV spike protein S from premature cleavage and increasing the efficacy of infective virion release from the cell (Westerbeck & Machamer, 2019). Successful expression of the protein E thus appears to be an essential requisite for pathogenesis; in fact attenuated SARS-CoV virions lacking E proteins have been suggested as vaccine candidates (Netland *et al.*, 2010). Viruses lacking both E and orf3a are not viable: Full-length E and orf3a proteins are required for maximal SARS-CoV

replication and virulence; in contrast, the viroporin orf8a has only a minor impact on these activities (Castaño-Rodriguez *et al.*, 2018).

E protein-mediated channel activity has been correlated with enhanced pulmonary damage following accumulation of liquid and electrolytes in pulmonary oedema observed in SARS, driven by the inflammasome NLRP3 and IL-1β overexpression (Nieto-Torres *et al.*, 2015). Porcine reproductive and respiratory syndrome virus infection also involves inflammasomes and IL 1β-induced inflammation and injury (Zhang *et al.*, 2013). This pathology could be related to the disruption of the epithelial apico-basal integrity in alveolar cells. In fact, SARS-CoV E protein has been shown to interact with PALS1, a tight-junction associated protein in mammalian cells (Teoh *et al.*, 2010). The interaction is mediated by a PDZ-binding motif at the carboxy-terminus of E that binds to a PDZ domain in PALS1. The authors speculate that SARS-CoV E hijacks PALS1 through this mechanism, abrogating epithelial cell differentiation, a phenomenon that could also occur in the alveolar cells in the pulmonary affectation of SARS (Teoh *et al.*, 2010) or SARS-CoV-2. In the case of mouse hepatitis virus (MHV), expression of E results in cellular apoptosis (Maeda *et al.*, 2001). The PDZ-binding motif in protein E, also present in the orf3a channel-forming protein, lends them the capacity to bind more than 400 target proteins in the infected host cells (Castaño-Rodriguez *et al.*, 2018), thus giving these viroporins sufficient versatility to perturb multiple aspects of normal cell function.

The E protein is probably involved in the neurotropism of CoVs. The human CoV HCoV-OC43 requires full expression of its E protein for efficient replication and

propagation in neuronal cells in culture and for neurovirulence in the central nervous system (Stodola *et al.*, 2018).

Therapeutic Potential of Channel Blockers Acting on CoV Ion Channels

The COVID-19 pandemic has given new impetus to research on the E protein of β-CoVs, the genus to which SARS-CoV-2 belongs. A genomic analysis of the entire database of β-CoVs showed that the gene coding for the E protein segregated into three different clusters, one of which includes only SARS-CoV, SARS-CoV-2, and two bat CoVs. SARS-CoV-2 E and the two bat CoVs are 100% identical, whereas E from SARS-CoV and SARS-CoV-2 show 95% homology (Alam *et al.*, 2020). The five C-terms of the homo-pentamer protrude into the cytoplasmic compartment, where three point-mutations (T55S, V56F, E69R) and a deletion (G70) mark the difference between the two latter viruses. The extremes of the C-term regions also harbour the loci of the key tetrapeptide segment (DLLV) involved in PDZ domain recognition (Alam *et al.*, 2020).

The ion channel function of SARS-CoV-2 E protein has recently been explored experimentally in bacteria using three indirect assays of channel activity: Growth deficiency upon overexpression, growth recovery in a K^+-uptake deficient *E. coli* strain, and cytoplasmic acidification in acidic growth media (Singh Tomar & Arkin, 2020). Exploring a library of repurposed drugs, these authors find that glicazide, of therapeutic application in type-2 diabetes mellitus, apparently blocks channel activity, as does the drug memantine. Memantine is a low-affinity, voltage-dependent, non-competitive antagonist of the glutamatergic NMDA receptor, the 5-HT3 receptor and the α7 nicotinic acetylcholine receptor -three members of the

pentameric ligand-gated ion channels (pLGIC)- and also an agonist of the dopamine D2 receptor. Memantine is used as a drug in Alzheimer disease, its therapeutic ability apparently residing in its channel-blocking activity. Using a prokaryotic model system, the proton- and GABA-gated pentameric ion channel protein GLIC from the bacterium *Gloeobacter violaceus*, Ulens and coworkers showed that memantine blocks channel activity by obstructing the channel vestibule facing the extracellular milieu (Ulens *et al.*, 2014).

The drug 5-N,N-hexamethylene amiloride has been shown to block the SARS-CoV E protein channel in a manner similar to the mechanism operating on the HIV-1 Vpu channel (Wilson *et al.*, 2006). Other viroporins -albeit from non-CoV viruses- have also been found to be potential targets of blocking compounds that interfere with assembly and release of mature virions (Behmard *et al.*, 2018).

Second to the large superfamily of G-protein coupled receptors (GPCR), ion channels are among the most sought-after membrane protein targets by the United States Federal Drug Administration. Ion channel modulators in particular have shown therapeutic potential and successes, e.g. as blockers of influenza M2 channels (Moorthy *et al.*, 2014, Sakai *et al.*, 2018, Niu *et al.*, 2019). It is expected that the current pandemic will prompt further research into this important area with obvious therapeutic opportunities.

Viral Ion Channel Proteins, Lipid Domains, and Evolution

As analysed in the preceding section, several drugs with pharmacological activity as ion channel blockers also inhibit ion fluxes mediated by viral ion channel proteins. Here I speculate on other possible common features between the two types of channels. It is estimated that about 4,000 million years ago planet Earth witnessed the appearance of

protein molecules with the capacity to selectively permeate ions through the plasma membranes of prokaryotic organisms like the cyanobacterium *Gloeobacter violaceus* or the bacillus *Erwinia chrysanthemi*. Comparison of the crystal structures of these proteins in Prokaryotes and their homologs in Eukaryotes has led to the notion that they belong to the same super-family of pLGICs (Tasneem *et al.*, 2005) that share a high degree of structural homology and phylogenetic conservation (Barrantes, 2015). Furthermore, scrutiny of the ion channel protein phylogeny disclosed interesting points of contact with the evolution of the machineries involved in lipid and in particular sterol biosynthesis. This observation led to the proposal of the possible co-evolution of the hopanoids (sterol surrogates) with ion channels in Prokaryotes and the appearance of sterols with ion channel proteins of Eukaryotes (Barrantes & Fantini, 2016).

The timing of appearance of viruses is still a controversial issue. Some evolutionists contend that viruses originated from 'ancient' cells that existed before the last universal cellular (common) ancestor (LUCA) gave rise to modern cells, i.e. to the three super-kingdoms of Archaea, Bacteria and Eukarya (Forterre, 2005), from ancient RNA cells that predated LUCA (Nasir *et al.*, 2020). In contrast, other theories support the idea that viruses evolved by recombination re-assortment of genes in a co-evolutionary process with cells rather than being ancestral to them (Hendrix *et al.*, 2000, Adachi *et al.*, 2020, Cui *et al.*, 2019). A third line of thought portrays the idea that viruses stem from cells via a process of reductive evolution, as hypothesized for giant DNA viruses (Koonin & Yutin, 2018). In the case of invertebrate viruses, co-evolution is supported by the large-effect polymorphisms for host resistance and viral evasion, which may have been favoured by virus-mediated selection (Obbard & Dudas, 2014).

Against this backdrop, an intriguing question is whether the cross-talk between channel protein motifs and microenvironmental lipids observed in higher cells also occurs in viral ion channel proteins. Indeed, the envelope lipid bilayer of influenza virus type A harbours cholesterol-rich, ordered lipid domains ("lipid rafts") (To & Torres, 2019), the characteristic lateral heterogeneities that are employed by eukaryotic cells as signalling platforms. Moreover, the cytoplasmic tail of influenza virus M2 binds human annexin A6, a Ca^{2+}/lipid-scaffold protein that interacts with ordered lipid domains and regulates cholesterol homeostatic equilibrium while it negatively modulates viral infection (Ma *et al.*, 2012). Similarly, a short linear motif in the cytoplasmic tail of influenza A M2 protein establishes interactions with another constitutive ordered lipid domain-resident protein, the cholesterol-binding protein caveolin-1; inhibition of caveolin-1 expression diminishes H1N1 influenza viral titres by hindering virus replication (Sun *et al.*, 2010). These may represent examples of molecular mimicry, where the virus appropriates cellular elements that enable it to interact with other endogenous partners of the host cell normally involved in physiological mechanisms, e.g. facilitating biogenesis, membrane association or trafficking of the virus among multiple other processes.

In the case of CoVs, lipid domains have been reported to serve as entry sites for SARS-CoV in Vero E6 cells (Lu *et al.*, 2008), possibly due to the enrichment of its receptor, ACE2, in these platforms; cholesterol depletion of ACE2-expressing cells by acute treatment with methyl-β-cyclodextrin reduced the binding of the S protein by 50% (Glende *et al.*, 2008). The α- and β-CoVs infect only mammals (Yu *et al.*, 2020) and may have appeared as variants of bat coronaviruses much more recently in evolutionary terms (Letko *et al.*, 2018, Cui *et al.*, 2019). All CoVs having orf3a structural homologs

evolved from the bat gene pool, whereas all those without the orf3a structural homologs derive from rodent, avian or pig gene pools (Kern *et al.*, 2020), suggesting coevolution of the ion channel protein orf3a in CoVs whose reservoir is the bat.

Another interesting case is provided by the similar structure and pharmacological sensitivity of the two pentameric viral ion channels, orf8a and E and the proton and GABA-sensitive prokaryotic channel GLIC. The pentameric bundle formed by the first 22 residues of the 39 amino acid-long SARS-CoV orf8a (Chen *et al.*, 2011) found a structural pattern on which to model it in the pentameric bundle of M2 helices of the bacterial GLIC protein from the cyanobacterium *Gloeobacter violaceus* (Hsu et al., 2015), a representative member of the superfamily of pLGICs (Nys *et al.*, 2013). Both orf8a and GLIC permeate chloride ions, and the Cl^- flux is voltage-sensitive (Hsu *et al.*, 2015). More remarkably, the GLIC prokaryotic ion channel is blocked with memantine (Ulens *et al.*, 2014), the same drug recently shown to inhibit the ion channel function of SARS-CoV-2 E protein (Singh Tomar & Arkin, 2020). Thus, the reported lack of homology between viral and prokaryotic/eukaryotic ion channels (McClenaghan *et al.*, 2020) may relate only to their primary sequence; their folding in space may provide the required 3D structure to constitute a binding site for small organic molecules acting as inhibitory drugs.

Knowledge of the phylogenetic kindredness between ion channel proteins of human pathogenic viruses and those of animal reservoirs may contribute not only to our understanding of the biology of the virus ion channels per se, but also to the development of therapeutic strategies to combat them. There are still many open avenues that could contribute to these endeavours and thus help prevent future

pandemics. Understanding the mechanisms of coronavirus ion channels is among these opportunities.

Future Directions in Viral Ion Channel Research

During recent months structural biology has made an unparalleled contribution to our understanding of the current pandemic. Biophysical approaches, exploiting previous methodological know-how and information accrued over the last two decades on other CoVs have produced new detailed data on the SARS-CoV-2 components (Barrantes, 2021). These help to shed light on the mechanisms involved in viral recognition by host-cell receptors and possible interventions to hinder this and other steps of the virus infective cycle. In comparison to the massive amount of data accrued on the S glycoprotein, viral ion channel proteins are still relatively unexplored both from the purely structural and mechanistic points of view. New structural data are needed to understand how viruses can alter the morphology of cellular components, modify the secretory vesicle transport system to subserve viral RNA replication, protect the spike S protein from premature cleavage, and efficiently assemble it into new virions through interaction with hijacked host-cell factors. A wide spectrum of techniques, and in particular the powerful cryo-EM, cryo-tomography, and superresolution optical microscopies offer new possibilities to investigate the viral ion channels with unprecedented resolution -atomic level in the case of cryo-EM and nanometric level (the mesoscale) in the case of live specimens studies with optical nanoscopy (Barrantes, 2021).

In addition, the very nature of viral ion channels makes it inherently possible, and will greatly benefit from, the application of a bifrontal approach combining the strengths of the structural cryo-imaging biophysical techniques (e.g., serial cryo-focused ion beam/scanning EM volume imaging) with single-molecule electrophysiology, in the form of single-channel patch-clamp recording of subcellular organelles, to characterize the structure-function correlations still missing to understand the pathogenic effects of the CoVs on cellular function.

Conflict of interests. The author declares no conflicts of interest.

Figures and figure legends

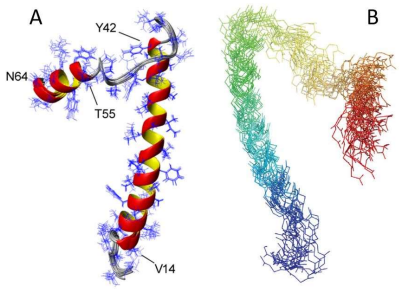

Figure 1. NMR work from the group of Torres led to the early models of the SARS-CoV E protein monomeric form in detergent-lipid micelles (Li *et al.*, 2014) showing two helical segments joined by a more disordered flexible region flanked by amino acid residues Y42 and T55 (A). The N-terminal portion of the TM region (indicated by residue V14 in (A)) is purported to protrude into the lumenal side of the Golgi membranes, and the C-terminal (here indicated by N64) to be partly exposed to the cytoplasm. (B) Subsequent work showed the calculated E monomers to consist of three α-helical segments in lauryl, myristoyl-phosphatidyl glycerol micelles (LMPG). The model shown corresponds to the ensemble of 10 calculated monomeric structures with the backbone rendered as a line representation Reproduced from ref. (Surya et al., 2018) with permission from Elsevier Masson SAS under Creative Commons Attribution license https://creativecommons.org/licenses/by/4.0

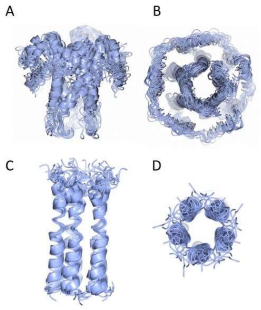

Figure 2. Comparative views of SARS-CoV and SARS-CoV-2 E protein models derived from NMR data. The t*op panel* shows the lowest-energy NMR-derived structural model of SARS-CoV E protein homo-pentamer (PDB 5X29) (Surya *et al.*, 2018) in lateral view (A) and end-on view (B). *Bottom panel*: NMR-derived model of SARS-CoV-2 E protein (PDB ID: 7K3G) (Mandala *et al.*, 2020) in lateral (C) and end-on (D) views. Notice that the ion channel-lining helices of SARS-CoV E run more perpendicular to the membrane plane in comparison to those of the SARS-CoV E protein. Images produced using the CCP4MG Molecular Graphics Program of the University of York, U.K.

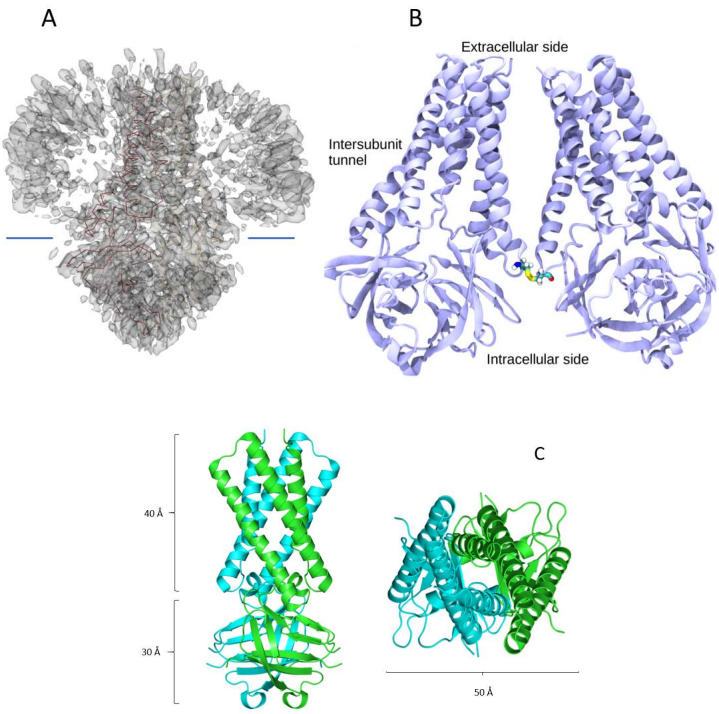

Figure 3. (A) Cryo-EM map at 2.9 Å resolution of full-length SARS-CoV-2 orf3a tetramer expressed in *Spodoptera frugiperda* and reconstituted in lipid nanodisks (Kern et al., 2020). The backbone chain of one of the protomers docked into the cryo-EM map is outlined in burgundy. The horizontal blue lines mark the limit between the upper TM domain and the lower cytoplasmic domain of the tetramer, formed by multiple β-sheets. (B) Ribbon model of SARS-CoV-2 orf3a tetramer derived from cryo-EM studies of the protein reconstituted in lipid nanodisks Each dimer possesses six TM helices and a cytoplasmic domain with predominantly β secondary structure. The two dimers in the tetramer are purported to be covalently joined by a disulphide bond formed by homologous Cys-133 residues in each monomer (Marquez-Miranda *et al.*, 2020). The molecular modelling study of these authors revealed the presence of a chloride ion site in the channel lumen. (C) Ribbon model of SARS-CoV-2 orf3a dimer, a ~70 Å cylinder in lateral view (*left*) and end-on perspective as viewed from the extracellular side (*right*) derived from cryo-EM studies of the protein reconstituted in lipid nanodisks (Kern *et al.*, 2020). Each protomer of the dimer has three helices that can fully traverse a lipid bilayer (~40 Å) and a 30 Å-long cytoplasmic domain with predominantly β secondary structure. The projection of the dimer onto the membrane plane is elliptic, with a major axis of ~50 Å in width. The central ion path is flanked by the TM segments 1 and 2, as seen in the centre of the end-on view. EMDB ID: EMD-

22136. Images produced using the CCP4MG Molecular Graphics Program of the University of York.

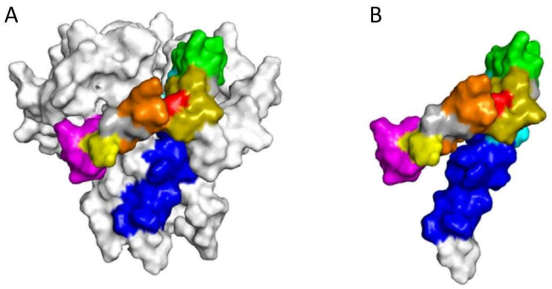

Figure 4. Putative surface epitopes of the SARS-CoV and SARS-CoV-2 E protein. A) Model of the homo-pentameric SARS-CoV E protein (PDB ID 5X29). Selected epitopes sequences are mapped in each monomer, displayed in (B). Epitope sequences are coloured as follow: blue: LIVNSVLLFLAFVVFLLVTLAILTALRLCAY; cyan: LLVTLAILTALRLCA; green: LTALRLCAY; olive green: CNIVNVSLVKPSFYV; red: SLVKPSFYV; orange: LVKPSFYVYSRVKNL; yellow: LVKPSFYVY; magenta: KPSFYVYSRVKNLNS. Reproduced from Fig. 2A,B of ref. (Tilocca *et al.*, 2020) with permission from Elsevier Masson SAS under Creative Commons Attribution license https://creativecommons.org/licenses/by/4.0.

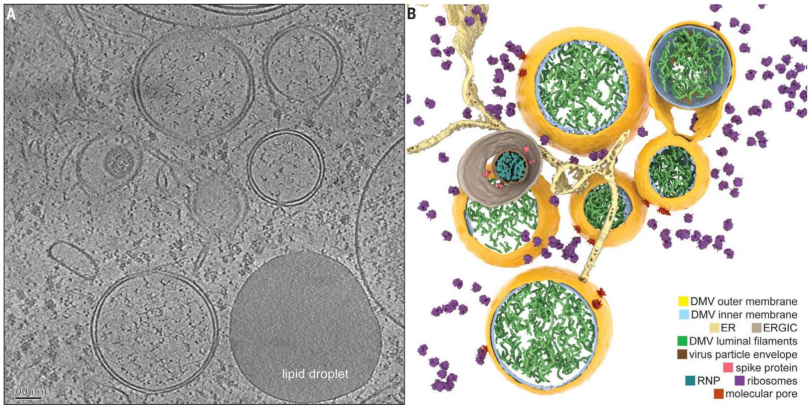

Figure 5. CoV-induced DMVs revealed by cryo-EM tomography. (A) Tomographic slice (7 nm thick) of a cryo-lamella milled through an MHV-infected cell at a middle stage of infection. (B) 3D model of the tomogram, with the segmented content annotated. ERGIC, ER-to-Golgi intermediate compartment. Reproduced from Figure 1

of ref. (Wolff *et al.*, 2020), with permission from the publisher under Creative Commons Attribution license https://creativecommons.org/licenses/by/4.0.

Reference List

Adachi, S., Koma, T., Doi, N., Nomaguchi, M. & Adachi, A. (2020). *Frontiers in immunology* **11**, 811.

Alam, I., Kamau, A. A., Kulmanov, M., Jaremko, Ł., Arold, S. T., Pain, A., Gojobori, T. & Duarte, C. M. (2020). *Front. Cell. Infect. Microbiol.* **10**, 405.

Almeida, J. D. & Tyrrell, D. A. (1967). *The Journal of general virology* **1**, 175-178.

Arbely, E., Khattari, Z., Brotons, G., Akkawi, M., Salditt, T. & Arkin, I. T. (2004). *J Mol Biol* **341**, 769-779.

Barrantes, F. J. (2015). *Biochimica et Biophysica Acta (BBA) - Biomembranes* **1848**, 1796-1805.

Barrantes, F. J. (2020). *Frontiers in physiology* **11**, 820.

Barrantes, F. J. (2021). *Annu Rev Biophys* **50**,

Barrantes, F. J. & Fantini, J. (2016). *Progress in lipid research* **63**, 1-13.

Behmard, E., Abdolmaleki, P. & Taghdir, M. (2018). *Biophysical chemistry* **233**, 47-54.

Cao, Y., Yang, R., Wang, W., Lee, I., Zhang, R., Zhang, W., Sun, J., Xu, B. & Meng, X. (2020). *Frontiers in molecular biosciences* **7**, 565797.

Castaño-Rodriguez, C., Honrubia, J. M., Gutiérrez-Álvarez, J., DeDiego, M. L., Nieto-Torres, J. L., Jimenez-Guardeño, J. M., Regla-Nava, J. A., Fernandez-Delgado, R., Verdia-Báguena, C., Queralt-Martín, M., Kochan, G., Perlman, S., Aguilella, V. M., Sola, I. & Enjuanes, L. (2018). *mBio* **9**, e02325-02317.

Cavasotto, C. N. & Di Filippo, J. I. (2021). *Molecular informatics* **40**, e2000115.

Cavasotto, C. N., Lamas, M. S. & Maggini, J. (2021). *European journal of pharmacology* **890**, 173705.

Chen, C.-C., Krüger, J., Sramala, I., Hsu, H.-J., Henklein, P., Chen, Y.-M. A. & Fischer, W. B. (2011). *Biochimica et Biophysica Acta (BBA) - Biomembranes* **1808**, 572-579.

Chen, S. C., Lo, S. Y., Ma, H. C. & Li, H. C. (2009). *Virus genes* **38**, 365-371.

Chien, T. H., Chiang, Y. L., Chen, C. P., Henklein, P., Hänel, K., Hwang, I. S., Willbold, D. & Fischer, W. B. (2013). *Biopolymers* **99**, 628-635.

Corse, E. & Machamer, C. E. (2000). **74**, 4319-4326.

Cui, J., Li, F. & Shi, Z. L. (2019). *Nature reviews. Microbiology* **17**, 181-192.

de Haan, C. A., Smeets, M., Vernooij, F., Vennema, H. & Rottier, P. J. (1999). *Journal of virology* **73**, 7441-7452.

DeDiego, M. L., Nieto-Torres, J. L., Jiménez-Guardeño, J. M., Regla-Nava, J. A., Alvarez, E., Oliveros, J. C., Zhao, J., Fett, C., Perlman, S. & Enjuanes, L. (2011). *PLoS pathogens* **7**, e1002315.

Díaz, J. (2020). *Frontiers in physiology* **11**, 870.

Estola, T. (1970). *Avian Diseases* **14**, 330-336.

Fischer, F., Stegen, C. F., Masters, P. S. & Samsonoff, W. A. (1998). *Journal of virology* **72**, 7885-7894.

Fischer, W. B. & Hsu, H.-J. (2011). *Biochimica et Biophysica Acta (BBA) - Biomembranes* **1808**, 561-571.

Forterre, P. (2005). *Biochimie* **87**, 793-803.

Freundt, E. C., Yu, L., Goldsmith, C. S., Welsh, S., Cheng, A., Yount, B., Liu, W., Frieman, M. B., Buchholz, U. J., Screaton, G. R., Lippincott-Schwartz, J., Zaki, S. R., Xu, X. N., Baric, R. S., Subbarao, K. & Lenardo, M. J. (2010). *Journal of virology* **84**, 1097-1109.

Fung, T. S. & Liu, D. X. (2019). *Annual review of microbiology* **73**, 529-557.

Glende, J., Schwegmann-Wessels, C., Al-Falah, M., Pfefferle, S., Qu, X., Deng, H., Drosten, C., Naim, H. Y. & Herrler, G. (2008). *Virology* **381**, 215-221.

Gonzalez, J. M., Gomez-Puertas, P., Cavanagh, D., Gorbalenya, A. E. & Enjuanes, L. (2003). *Archives of virology* **148**, 2207-2235.

Guan, W. J., Ni, Z. Y., Hu, Y., Liang, W. H., Ou, C. Q., He, J. X., Liu, L., Shan, H., Lei, C. L., Hui, D. S. C., Du, B., Li, L. J., Zeng, G., Yuen, K. Y., Chen, R. C., Tang, C. L., Wang, T., Chen, P. Y., Xiang, J., Li, S. Y., Wang, J. L., Liang, Z. J., Peng, Y. X., Wei, L., Liu, Y., Hu, Y. H., Peng, P., Wang, J. M., Liu, J. Y., Chen, Z., Li, G., Zheng, Z. J., Qiu, S. Q., Luo, J., Ye, C. J., Zhu, S. Y. & Zhong, N. S. (2020). *The New England journal of medicine* **382**, 1708-1720.

Harrison, S. C. (2015). *Virology* **479-480**, 498-507.

Hartley, J. W., Rowe, W. P., Bloom, H. H. & Turner, H. C. (1964). *Proceedings of the Society for Experimental Biology and Medicine. Society for Experimental Biology and Medicine (New York, N.Y.)* **115**, 414-418.

Hendrix, R. W., Lawrence, J. G., Hatfull, G. F. & Casjens, S. (2000). *Trends in microbiology* **8**, 504-508.

Hsu, H. J., Lin, M. H., Schindler, C. & Fischer, W. B. (2015). *Proteins* **83**, 300-308.
Ke, Z., Oton, J., Qu, K., Cortese, M., Zila, V., McKeane, L., Nakane, T., Zivanov, J., Neufeldt, C. J., Cerikan, B., Lu, J. M., Peukes, J., Xiong, X., Kräusslich, H. G., Scheres, S. H. W., Bartenschlager, R. & Briggs, J. A. G. (2020). *Nature* **588**, 498-502.
Kern, D. M., Sorum, B., Hoel, C. M., Sridharan, S., Remis, J. P., Toso, D. B. & Brohawn, S. G. (2020). 2020.2006.2017.156554.
Koonin, E. V. & Yutin, N. (2018). *F1000Research* **7**, 16248.16241.
Lai, M. M. & Cavanagh, D. (1997). *Advances in virus research* **48**, 1-100.
Letko, M., Miazgowicz, K., McMinn, R., Seifert, S. N., Sola, I., Enjuanes, L., Carmody, A., van Doremalen, N. & Munster, V. (2018). *Cell Rep* **24**, 1730-1737.
Li, X., Giorgi, E. E., Marichannegowda, M. H., Foley, B., Xiao, C., Kong, X.-P., Chen, Y., Gnanakaran, S., Korber, B. & Gao, F. (2020). *Science advances* **6**, eabb9153.
Li, Y., Surya, W., Claudine, S. & Torres, J. (2014). *J. Biol. Chem.* **289**, 12535-12549.
Liao, Y., Fung, T. S., Huang, M., Fang, S. G., Zhong, Y. & Liu, D. X. (2013). *Journal of virology* **87**, 8124-8134.
Liao, Y., Lescar, J., Tam, J. P. & Liu, D. X. (2004). *Biochemical and biophysical research communications* **325**, 374-380.
Liao, Y., Tam, J. P. & Liu, D. X. (2006). *Advances in experimental medicine and biology* **581**, 199-202.
Lim, K. P., Xu, H. Y. & Liu, D. X. (2001). *Advances in experimental medicine and biology* **494**, 595-602.
Lu, W., Zheng, B. J., Xu, K., Schwarz, W., Du, L., Wong, C. K., Chen, J., Duan, S., Deubel, V. & Sun, B. (2006). *Proceedings of the National Academy of Sciences of the United States of America* **103**, 12540-12545.
Lu, Y., Liu, D. X. & Tam, J. P. (2008). *Biochemical and biophysical research communications* **369**, 344-349.
Ma, H., Kien, F., Manière, M., Zhang, Y., Lagarde, N., Tse, K. S., Poon, L. L. M. & Nal, B. (2012). *J. Virol.* **86**, 1789-1801.
Madan, V., García Mde, J., Sanz, M. A. & Carrasco, L. (2005). *FEBS letters* **579**, 3607-3612.
Maeda, J., Repass, J. F., Maeda, A. & Makino, S. (2001). *Virology* **281**, 163-169.
Mandala, V. S., McKay, M. J., Shcherbakov, A. A., Dregni, A. J., Kolocouris, A. & Hong, M. (2020). *Nature Structural & Molecular Biology* **27**, 1202-1208.
Marquez-Miranda, V., Rojas, M., Duarte, Y., Diaz-Franulic, I., Holmgren, M., Cachau, R. & Gonzalez-Nilo, F. D. (2020). 2020.2010.2022.349522.
McClenaghan, C., Hanson, A., Lee, S.-J. & Nichols, C. G. (2020). *Front. Immunol.* **11**, 573339.
Minakshi, R., Padhan, K., Rani, M., Khan, N., Ahmad, F. & Jameel, S. (2009). *PloS one* **4**, e8342.
Moorthy, N. S., Poongavanam, V. & Pratheepa, V. (2014). *Mini reviews in medicinal chemistry* **14**, 819-830.
Nasir, A., Romero-Severson, E. & Claverie, J.-M. (2020). *Trends in microbiology* **28**, 959-967.
Netland, J., DeDiego, M. L., Zhao, J., Fett, C., Álvarez, E., Nieto-Torres, J. L., Enjuanes, L. & Perlman, S. (2010). *Virology* **399**, 120-128.
Neuman, B. W., Adair, B. D., Yoshioka, C., Quispe, J. D., Orca, G., Kuhn, P., Milligan, R. A., Yeager, M. & Buchmeier, M. J. (2006). *Journal of virology* **80**, 7918-7928.
Neuman, B. W. & Buchmeier, M. J. (2016). *Advances in virus research* **96**, 1-27.
Neuman, B. W., Kiss, G., Kunding, A. H., Bhella, D., Baksh, M. F., Connelly, S., Droese, B., Klaus, J. P., Makino, S., Sawicki, S. G., Siddell, S. G., Stamou, D. G., Wilson, I. A., Kuhn, P. & Buchmeier, M. J. (2011). *Journal of structural biology* **174**, 11-22.
Nieto-Torres, J. L., Verdiá-Báguena, C., Jimenez-Guardeño, J. M., Regla-Nava, J. A., Castaño-Rodriguez, C., Fernandez-Delgado, R., Torres, J., Aguilella, V. M. & Enjuanes, L. (2015). *Virology* **485**, 330-339.
Niu, T., Zhao, X., Jiang, J., Yan, H., Li, Y., Tang, S., Li, Y. & Song, D. (2019). *Molecules (Basel, Switzerland)* **24**, 921.
Nys, M., Kesters, D. & Ulens, C. (2013). *Biochemical pharmacology* **86**, 1042-1053.
Obbard, D. J. & Dudas, G. (2014). *Curr Opin Virol* **8**, 73-78.
OuYang, B. & Chou, J. J. (2014). *Biochimica et Biophysica Acta (BBA) - Biomembranes* **1838**, 1058-1067.
Pervushin, K., Tan, E., Parthasarathy, K., Lin, X., Jiang, F. L., Yu, D., Vararattanavech, A., Soong, T. W., Liu, D. X. & Torres, J. (2009). *PLoS pathogens* **5**, e1000511.
Pinto, L. H., Holsinger, L. J. & Lamb, R. A. (1992). *Cell* **69**, 517-528.
Raamsman, M. J., Locker, J. K., de Hooge, A., de Vries, A. A., Griffiths, G., Vennema, H. & Rottier, P. J. (2000). *Journal of virology* **74**, 2333-2342.
Ren, Y., Shu, T., Wu, D., Mu, J., Wang, C., Huang, M., Han, Y., Zhang, X. Y., Zhou, W., Qiu, Y. & Zhou, X. (2020). *Cellular & molecular immunology* **17**, 881-883.

Richardson, S., Hirsch, J. S., Narasimhan, M., Crawford, J. M., McGinn, T., Davidson, K. W. & Consortium, a. t. N. C.-R. (2020). *JAMA* **323**, 2052-2059.
Sakai, Y., Kawaguchi, A., Nagata, K. & Hirokawa, T. (2018). *Microbiology and immunology* **62**, 34-43.
Scheller, C., Krebs, F., Minkner, R., Astner, I., Gil-Moles, M. & Wätzig, H. (2020). *Electrophoresis* **n/a**, 1-10.
Schoeman, D. & Fielding, B. C. (2019). *Virology journal* **16**, 69.
Shen, S., Lin, P. S., Chao, Y. C., Zhang, A., Yang, X., Lim, S. G., Hong, W. & Tan, Y. J. (2005). *Biochemical and biophysical research communications* **330**, 286-292.
Singh Tomar, P. P. & Arkin, I. T. (2020). *Biochemical and biophysical research communications* **530**, 10-14.
Siu, Y. L., Teoh, K. T., Lo, J., Chan, C. M., Kien, F., Escriou, N., Tsao, S. W., Nicholls, J. M., Altmeyer, R., Peiris, J. S. M., Bruzzone, R. & Nal, B. (2008). **82**, 11318-11330.
Snijder, E. J., Limpens, R., de Wilde, A. H., de Jong, A. W. M., Zevenhoven-Dobbe, J. C., Maier, H. J., Faas, F., Koster, A. J. & Bárcena, M. (2020). *PLoS Biol* **18**, e3000715.
Stodola, J. K., Dubois, G., Le Coupanec, A., Desforges, M. & Talbot, P. J. (2018). *Virology* **515**, 134-149.
Su, S., Wong, G., Shi, W., Liu, J., Lai, A. C. K., Zhou, J., Liu, W., Bi, Y. & Gao, G. F. (2016). *Trends in microbiology* **24**, 490-502.
Sun, L., Hemgård, G.-V., Susanto, S. A. & Wirth, M. (2010). *Virology journal* **7**, 108.
Surya, W., Li, Y. & Torres, J. (2018). *Biochimica et biophysica acta. Biomembranes* **1860**, 1309-1317.
Surya, W., Li, Y., Verdià-Bàguena, C., Aguilella, V. M. & Torres, J. (2015). *Virus Res* **201**, 61-66.
Tan, Y. J., Teng, E., Shen, S., Tan, T. H., Goh, P. Y., Fielding, B. C., Ooi, E. E., Tan, H. C., Lim, S. G. & Hong, W. (2004). *Journal of virology* **78**, 6723-6734.
Tan, Y. J., Tham, P. Y., Chan, D. Z., Chou, C. F., Shen, S., Fielding, B. C., Tan, T. H., Lim, S. G. & Hong, W. (2005). *Journal of virology* **79**, 10083-10087.
Tasneem, A., Iyer, L. M., Jakobsson, E. & Aravind, L. (2005). *Genome Biol.* **6**, R4.
Teoh, K.-T., Siu, Y.-L., Chan, W.-L., Schlüter, M. A., Liu, C.-J., Peiris, J. S. M., Bruzzone, R., Margolis, B. & Nal, B. (2010). **21**, 3838-3852.
Tilocca, B., Soggiu, A., Sanguinetti, M., Babini, G., De Maio, F., Britti, D., Zecconi, A., Bonizzi, L., Urbani, A. & Roncada, P. (2020). *Microbes and Infection* **22**, 182-187.
To, J., Surya, W., Fung, T. S., Li, Y., Verdià-Bàguena, C., Queralt-Martin, M., Aguilella, V. M., Liu, D. X. & Torres, J. (2017). *Journal of virology* **91**, e02158-02116.
To, J., Surya, W. & Torres, J. (2016). *Advances in protein chemistry and structural biology*, edited by R. Donev, pp. 307-355: Academic Press.
To, J. & Torres, J. (2019). *Cells* **8**, 654.
Torres, J., Wang, J., Parthasarathy, K. & Liu, D. X. (2005). *Biophysical journal* **88**, 1283-1290.
Tortorici, M. A. & Veesler, D. (2019). *Advances in virus research* **105**, 93-116.
Ulens, C., Spurny, R., Thompson, Andrew J., Alqazzaz, M., Debaveye, S., Han, L., Price, K., Villalgordo, Jose M., Tresadern, G., Lynch, Joseph W. & Lummis, Sarah C. R. (2014). *Structure* **22**, 1399-1407.
Unchwaniwala, N., Zhan, H., Pennington, J., Horswill, M., den Boon, J. A. & Ahlquist, P. (2020). *Proceedings of the National Academy of Sciences of the United States of America* **117**, 18680-18691.
Venkatagopalan, P., Daskalova, S. M., Lopez, L. A., Dolezal, K. A. & Hogue, B. G. (2015). *Virology* **478**, 75-85.
Verdiá-Báguena, C., Nieto-Torres, J. L., Alcaraz, A., DeDiego, M. L., Enjuanes, L. & Aguilella, V. M. (2013). *Biochimica et Biophysica Acta (BBA) - Biomembranes* **1828**, 2026-2031.
Verdiá-Báguena, C., Nieto-Torres, J. L., Alcaraz, A., DeDiego, M. L., Torres, J., Aguilella, V. M. & Enjuanes, L. (2012). *Virology* **432**, 485-494.
Wang, K., Lu, W., Chen, J., Xie, S., Shi, H., Hsu, H., Yu, W., Xu, K., Bian, C., Fischer, W. B., Schwarz, W., Feng, L. & Sun, B. (2012). *FEBS letters* **586**, 384-391.
Westerbeck, J. W. & Machamer, C. E. (2019). *Journal of virology* **93**, e00015-00019.
Wilson, L., Gage, P. & Ewart, G. (2006). *Virology* **353**, 294-306.
Wilson, L., McKinlay, C., Gage, P. & Ewart, G. (2004). *Virology* **330**, 322-331.
Wolff, G., Limpens, R. W. A. L., Zevenhoven-Dobbe, J. C., Laugks, U., Zheng, S., de Jong, A. W. M., Koning, R. I., Agard, D. A., Grünewald, K., Koster, A. J., Snijder, E. J. & Bárcena, M. (2020). *Science (New York, N.Y.)* **369**, 1395-1398.
Woo, P. C. Y., Lau, S. K. P., Lam, C. S. F., Tsang, A. K. L., Hui, S.-W., Fan, R. Y. Y., Martelli, P. & Yuen, K.-Y. (2014). *J Virol* **88**, 1318-1331.
Wrapp, D., Wang, N., Corbett, K. S., Goldsmith, J. A., Hsieh, C. L., Abiona, O., Graham, B. S. & McLellan, J. S. (2020). *Science (New York, N.Y.)* **367**, 1260-1263.

Wu, Q., Zhang, Y., Lü, H., Wang, J., He, X., Liu, Y., Ye, C., Lin, W., Hu, J., Ji, J., Xu, J., Ye, J., Hu, Y., Chen, W., Li, S., Wang, J., Wang, J., Bi, S. & Yang, H. (2003). *Genomics, proteomics & bioinformatics* **1**, 131-144.

Yan, H., Xiao, G., Zhang, J., Hu, Y., Yuan, F., Cole, D. K., Zheng, C. & Gao, G. F. (2004). *J. Med. Virol.* **73**, 323-331.

Ye, Y. & Hogue, B. G. (2007). *J. Virol.* **81**, 3597-3607.

Yu, J., Qiao, S., Guo, R. & Wang, X. (2020). *Nature Communications* **11**, 3070.

Zhang, K., Hou, Q., Zhong, Z., Li, X., Chen, H., Li, W., Wen, J., Wang, L., Liu, W. & Zhong, F. (2013). *Virology* **442**, 156-162.

Zhang, R., Wang, K., Lv, W., Yu, W., Xie, S., Xu, K., Schwarz, W., Xiong, S. & Sun, B. (2014). *Biochimica et Biophysica Acta (BBA) - Biomembranes* **1838**, 1088-1095.